International Journal of Pharmaceutics 496 (2015) 291–298

Contents lists available at ScienceDirect

International Journal of Pharmaceutics

journal homepage: www.elsevier.com/locate/ijpharm

Drug release from slabs and the effects of surface roughness

George Kalosakas[a,b,*], Dimitra Martini[c]

[a] University of Patras, Materials Science Dept., Rio GR-26504, Greece
[b] Crete Center for Quantum Complexity and Nanotechnology (CCQCN), Physics Dept., University of Crete, 71003 Heraklion, Greece
[c] University of Patras, Rio GR-26504, Greece

ARTICLE INFO

Article history:
Received 28 August 2015
Accepted 3 October 2015
Available online 8 October 2015

Keywords:
Controlled drug release
Slabs/thin films
Surface roughness
Diffusion
Monte Carlo simulations
Stretched exponential release curves

ABSTRACT

We discuss diffusion-controlled drug release from slabs or thin films. Analytical and numerical results are presented for slabs with flat surfaces, having a uniform thickness. Then, considering slabs with rough surfaces, the influence of a non-uniform slab thickness on release kinetics is numerically investigated. The numerical release profiles are obtained using Monte Carlo simulations. Release kinetics is quantified through the stretched exponential (or Weibull) function and the resulting dependence of the two parameters of this function on the thickness of the slab, for flat surfaces, and the amplitude of surface fluctuations (or the degree of thickness variability) in case of roughness. We find that a higher surface roughness leads to a faster drug release.

1. Introduction

There are many applications of drug or biomolecular release from slabs, thin films or multilayers, and membranes. A few recent examples report: nanostructured films exhibiting lysozyme-controlled release of EGF for wound-healing applications [1], sol–gel silica thin films providing efficient local delivery of antibiotics with adjuvant for potential inhibition of bacterial infection in titanium implants [2], multilayered films sequentially releasing multiple drugs for periodontitis treatment [3], multilayers showing suppression of burst release and an adjustable release rate regulated by the composition and the relative thickness of the layers [4], etc.

Theoretical modeling is simplified in such systems due to the one-dimensional character of the device, since release from the edges is considered negligible. The release predominantly occurs through the main surfaces of the slab, which are very large in size compared to the corresponding thickness, while release from the other directions is ignored. Furthermore, edge effects near the boundaries of the main surfaces can be neglected. Thus, the relevant spatial variable is the one along the direction perpendicular to these surfaces.

The celebrated Higuchi model [5] (see also the review [6]) refers to such a one-dimensional formulation. Several reviews [7–11], as well as seminal papers [12,13], discuss the corresponding equations and present analytical results for devices having a slab shape. As it has been nicely shown in Ref. [14], the simplicity of such geometries and the availability of analytical solutions of diffusion equation can be efficiently used for the determination of the diffusion coefficient of a drug of interest, by fitting the analytical results with experimental release profiles of appropriately prepared thin films. Apart from the simpler cases, described merely by diffusion, models dealing with more complex situations including swelling [15–17] or degradation [18–20], have been considered too for one-dimensional planar geometries.

Here we investigate the effects of the roughness of slab's surfaces on drug release profiles. We consider diffusion-controlled drug release, where swelling or degradation/erosion phenomena are not significant. Therefore, stationary surface boundaries, either flat or irregular, interfacing the release medium are used. First we quantify release kinetics for slabs with smooth flat surfaces, presenting a uniform thickness. Numerically obtained release profiles, through Monte Carlo simulations, are compared with predictions from the analytical solution of diffusion equation. Then, slabs with irregular, rough surfaces are examined. The thickness of the slab is non-uniform in this case; it exhibits variations around an average value. We present the dependence of Monte Carlo calculated release curves on the amplitude of surface fluctuations, which serves as a measure of the irregularity of the surfaces of the slab and the corresponding variability of its thickness.

In all cases release kinetics is quantified using the stretched exponential function, known as Weibull function too. Thus, release

* Corresponding author at: University of Patras, Materials Science Dept., Rio GR-26504, Greece.
E-mail address: georgek@upatras.gr (G. Kalosakas).

http://dx.doi.org/10.1016/j.ijpharm.2015.10.018
0378-5173/

profiles are fitted with the equation [21]:

$$\frac{M_t}{M_\infty} = 1 - \exp\left[-\left(\frac{t}{\tau}\right)^b\right] \quad (1)$$

where M_t is the amount of drug released at time t, M_∞ is the total amount of drug released at infinite time, and b, τ are the two parameters of the function. The stretched exponential function, Eq. (1), has been extensively used to describe both experimental [22,23,1] and numerical [24–33] release data.

2. Methods

2.1. Monte Carlo simulations for slabs with flat surfaces (uniform thickness)

We consider a slab of uniform thickness L, lying on the xy-plane (i.e., its two main surfaces are parallel to the xy-plane, at a vertical distance L), where the drug is released along the direction of z-axis.

Monte Carlo simulations of drug release are performed using a three-dimensional lattice consisting of $N_x \times N_y \times N_z$ sites [24,32]. Initially a number N_0 of drug particles ($N_0 \leq N_x N_y N_z$) are randomly placed on lattice cells, avoiding double occupancy (as excluded volume interactions are assumed between the particles). The number of particles N_0 is related to the desired loading concentration C_0 (which equals to $C_0 = N_0/N_x N_y N_z$).

During the numerical simulation, at each Monte Carlo step a drug particle is randomly chosen. Then one of its six neighboring lattice sites is randomly selected and if this site is empty then the chosen particle is moved there. Otherwise, if the selected neighboring site is already occupied by another particle, then the chosen particle remains at its position.

A drug particle is released during the simulation whenever both conditions are met: (i) the particle occupies a lattice site belonging either to upper, or to the lower, main surface of the slab (located at $z = L$, or $z = 0$, respectively) *and* (ii) the randomly selected neighboring site is upwards, or downwards, respectively. Release is not permitted from the other faces of the lattice, by considering periodic boundary conditions at the x- and y- axes. For example, if a particle lies at the left boundary of the lattice (at $x = 0$) and the randomly selected neighboring site is towards the left, then the particle re-enters from the opposite face of the lattice (at the right boundary) with the same y and z coordinates (provided of course that this new site is empty, otherwise the particle stays at its initial position). Similar considerations hold for the right boundary of the lattice, as well as for the two other boundaries perpendicular to the y-axis.

The number of drug particles $N(t)$ remaining in the lattice is monitored during the simulation. Monte Carlo time t is increased by $1/N(t)$ at each Monte Carlo step. A simulation stops when all drug particles are released and the lattice is empty. Release profiles M_t/M_∞ are obtained by statistically averaging the quantity $\frac{N_0 - N(t)}{N_0}$ over a number R_s of different realizations (i.e., different random simulations as described above) at each case.

2.2. Monte Carlo simulations for slabs with rough surfaces (non-uniform thickness)

In this case the upper and lower surfaces (drug releasing boundaries) of the lattice representing the slab are no longer flat, but they are irregular. To quantify the roughness of slab's surfaces we introduce a parameter w, representing the amplitude of the fluctuations of each surface.

We numerically construct lattices with irregular upper (lower) surfaces lying in the region $L \pm w$ ($0 \pm w$) of the z-axis, instead of being fixed at the constant value $z = L$ ($z = 0$) as happened previously. Let us consider the two-dimensional $N_x \times N_y$ grid of the lattice points at the xy-plane. At each point i, j of this grid the corresponding z coordinate of the upper (lower) surface may now have a different value $zu_{i,j}$ ($zl_{i,j}$), with $L - w \leq zu_{i,j} \leq L + w$ ($-w \leq zl_{i,j} \leq w$). The thickness of the slab at each point i,j of this grid is $L_{i,j} = zu_{i,j} - zl_{i,j}$, with $L_{i,j}$ taking values in the region from $L - 2w$ to $L + 2w$. (In the case of flat surfaces considered in the previous subsection, it was $zu_{i,j} = L$ and $zl_{i,j} = 0$ for all points i,j of the grid, leading to a uniform slab thickness $L_{i,j} = L$ everywhere).

In order to avoid abrupt variations of the position of the upper and lower surface at each point i,j of the grid, we consider a regularly spaced sub-grid formed every a number n_s of the $N_x \times N_y$ lattice points, as shown by red squares in Fig. S1 of the Supplementary information ($n_s = 5$ in that case). At each point of this sub-grid a random integer number, homogeneously distributed in the region $L \pm w$ ($0 \pm w$), is selected for the z coordinate zu (zl) of the upper (lower) surface. Then bilinear interpolation between these random values is used for obtaining the integer values corresponding to the z coordinates of the upper or lower surface at the other points of the $N_x \times N_y$ grid. Using this procedure rough slab surfaces are numerically constructed, with positions varying in a range of $2w$ (see Fig. 4a and b below). The resulted slabs present non-uniform thickness in the interval $L \pm \Delta L$ (see Fig. 5a), with $\Delta L = 2w$ the degree of thickness variability. The values of the thickness of the slab obtained in this way show a Gaussian-like distribution around the mean thickness L, with a width provided through ΔL (see Fig. 5b).

The Monte Carlo simulations are performed as previously, with the difference now that the drug particles are randomly moving on a lattice with irregular upper and lower surfaces as described above. Here a drug particle can be released by the upper (lower) non-planar surface not only by moving upwards (downwards), as previously, but also if it is randomly selected to move along the direction of x- or y-axis in the case that the corresponding neighboring site lies outside of the considered lattice sites representing the slab, due to the roughness of the surface. For the statistical average of the release profiles in this case, different irregular surfaces, corresponding to a particular L and w, are constructed at each realization.

3. Results and discussion

3.1. Drug release from slabs with flat surfaces

3.1.1. Predictions from the analytical solution of diffusion equation

The equation of Fick's second law can be easily solved for a slab with planar surfaces, thickness L, and drug diffusion coefficient D. In this case the problem is reduced to the one-dimensional diffusion equation. Considering homogeneously distributed drug particles as initial condition and sink boundary conditions, the obtained fractional release is

$$\frac{M_t}{M_\infty} = 1 - \frac{8}{\pi^2}\sum_{n=0}^{\infty}\frac{1}{(2n+1)^2}\exp\left(-(2n+1)^2\pi^2\frac{D}{L^2}t\right) \quad (2)$$

The analysis is simplified using the dimensionless time $t_d = Dt/L^2$. Then Eq. (2) yields

$$\frac{M_t}{M_\infty} = 1 - \frac{8}{\pi^2}\sum_{n=0}^{\infty}\frac{1}{(2n+1)^2}\exp\left(-(2n+1)^2\pi^2 t_d\right) \quad (3)$$

There is not any parameter in the solution now, as the device characteristics are hidden in the units of time. We fit this solution with the stretched exponential release, Eq. (1), since the latter

provides a more convenient analytical description. Moreover, in this way we can compare the analytical predictions with the corresponding numerical simulations presented next.

The plot of Eq. (3) is shown in Fig. 1 with circles, along with the corresponding fitting (solid line) by the stretched exponential Eq. (1). The fitted parameters are $b = 0.80$ and the dimensionless time parameter $\tau_d = 0.076$. Note from Eq. (1) that the stretched exponential parameter τ has units of time, while b is dimensionless. Taking into account that $\tau_d = D\tau/L^2$, we obtain the following predictions from the analytical solution of diffusion equation:

$$\tau = 0.076\frac{L^2}{D} \tag{4}$$

$$b = 0.80 \tag{5}$$

We see that both parameters do not depend on the initial drug concentration C_0, while b is also predicted to be independent on the other device characteristics, L and D. These results are similar to those obtained in the case of release from spherical devices [32].

The obtained value of b in Eq. (5) agrees very well with a suggested relation [22] between the stretched exponential exponent and the exponent n appearing in the well known Peppas power-law: $M_t/M_\infty = kt^n$. For Fickian release from slabs, the exponent in the latter formula equals to $n = 0.5$ [12]. Analyzing a large number of data in Ref. [22], the linear relationship $b = 1.4n + 0.11$ has been suggested. For $n = 0.5$ this equation yields $b = 0.81$.

3.1.2. Numerical results obtained by Monte Carlo simulations

Here we discuss results for drug release from slabs with planar surfaces, obtained by Monte Carlo simulations. For the data presented below we have used $R_s = 100$ different realizations in lattices with $N_x = N_y = 20$ sites in the x and y directions where the periodic boundary conditions are used (see Subsection 2.1). We have checked in indicative cases that the same results are obtained using 200 realizations and lattices with $N_x = N_y = 10$ or 40 sites.

We first examine the potential dependence of release profiles on the initial concentration C_0 of the drug. Values of C_0 ranging from 4% to 50% are used. As expected, release kinetics does not depend on C_0. This is in agreement with the results of similar studies in other systems [24,32,33], as well as with the analytical predictions from the diffusion equation.

Then the influence of the thickness L of the slab on the release is investigated. Circles in Fig. 2 show the fractional release obtained for various values of thickness from $L = 10$ up to $L = 100$. Here L is measured in units of the lattice spacing l_u [32], and therefore its value coincides with N_z. We see from Fig. 2 that release is delayed for thicker slabs, as anticipated. We use the stretched exponential function, Eq. (1), to quantify the observed behavior.

Solid lines in Fig. 2 present fittings of the numerical release profiles with Eq. (1). From these fittings the stretched exponential parameters b and τ are obtained for different values of L. These dependencies are shown by symbols in Fig. 3: the time parameter τ is proportional to L^2, as it can be seen by the fitting with the parabolic solid line showing the relation $\tau = 0.48L^2$, while the exponent b is inversely proportional to L as shows the corresponding linear fitting of $b = f(1/L)$ with the solid line $b = 0.71 + \frac{1.1}{L}$.

The above mentioned relations, obtained through the fittings shown in Fig. 3, concern dimensionless quantities. For a discussion of the units of length, l_u, and time, t_u, considered in the Monte Carlo simulations see the relevant discussion in Ref. [32]. Taking into account dimensional analysis regarding the dependence of time parameter τ on the thickness L and the drug diffusion coefficient D and also that the diffusion coefficient corresponding to the Monte Carlo process described in Subsection 2.1 equals to $l_u^2/6t_u$ [32], one then obtains that in normal units

$$\tau = \frac{0.48L^2}{6\ D} = 0.080\frac{L^2}{D} \tag{6}$$

This relation, derived from the numerical simulations, is in close agreement with Eq. (4) predicted from the analytical solution of Fick's second law.

The dependence of b on thickness L in normal units reads

$$b = 0.71 + \frac{1.1}{L/l_u} \approx 0.71 \tag{7}$$

Since l_u is assumed to be of the order of the linear dimensions of drug particles, the thickness of the slab is much larger than that, i.e., $L >> l_u$. This implies that the second term $\frac{1.1}{L/l_u}$ of the sum in the last equation can be neglected, resulting in a constant value of b, in

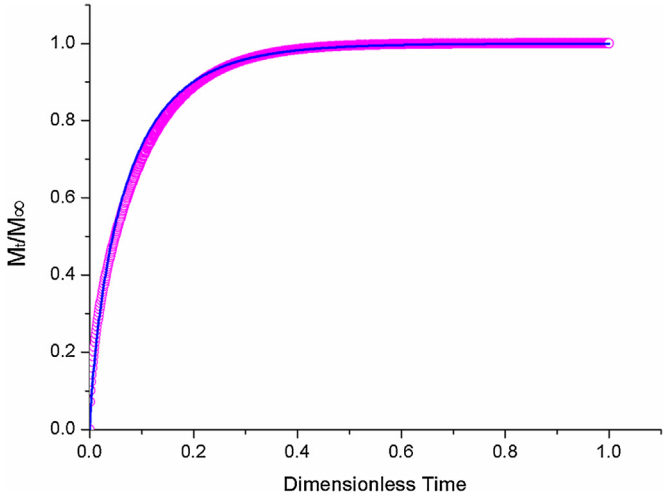

Fig. 1. The release profile, M_t/M_∞, as a function of the dimensionless time $t_d = Dt/L^2$, obtained from the analytical solution, Eq. (3), of diffusion equation for the case of a slab (magenta circles). Continuous blue line shows the fitting with the stretched exponential function, Eq. (1), resulting in $b = 0.80$ and $\tau_d = 0.076$.

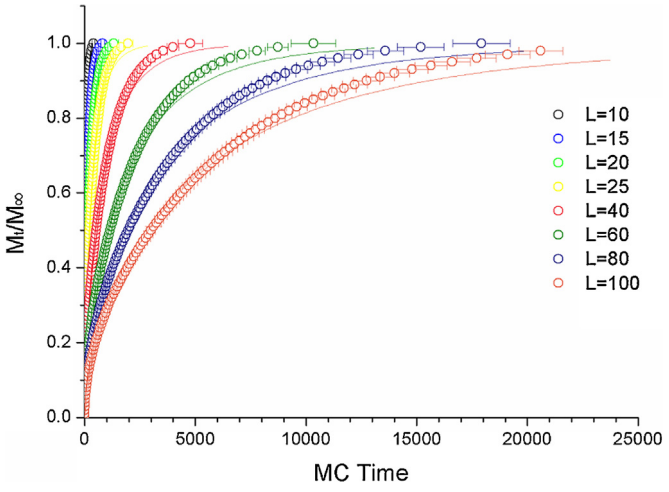

Fig. 2. Release profiles, M_t/M_∞, as a function of Monte Carlo time for slabs of different thickness L (circles). Error bars correspond to standard deviations from the different realizations. Solid lines represent fittings of the numerical results with the stretched exponential function, Eq. (1).

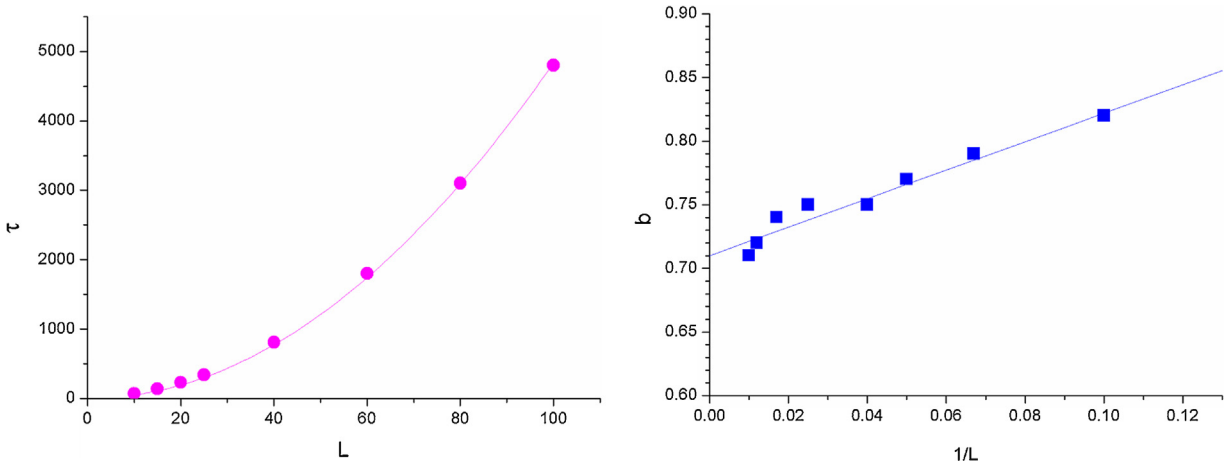

Fig. 3. Dependence of the stretched exponential parameters τ and b on the thickness L of the slab, as obtained through the fittings of the numerical results of Fig. 2 with Eq. (1). *Left*: τ as a function of L (circles). Solid line shows a fitting with a parabolic function $\tau \sim L^2$. *Right*: b as a function of $1/L$ (squares). Solid line shows a linear fitting.

accordance with the analytical prediction. However, the constant term is somewhat smaller than that of Eq. (5).

Similar dependencies of the stretched exponential parameters b and τ as those of Eqs. (6) and (7), have been numerically found in the case of release from spheres too, with the radius of the sphere replacing the thickness L (see Eqs. (11) and (13) in Ref. [32]). As happens in the case of spheres, also here, for slabs, the proportionality coefficient in τ (the constant term in b) is around 6% larger (10% smaller) than the corresponding prediction of the analytical solution of diffusion equation. Note at this point that the used Monte Carlo simulations take into account excluded volume interactions between the diffusive drug particles, while no interactions are considered in the analytical treatment of diffusion equation. However, it has been surprisingly found that Monte Carlo simulations produce the same results regardless whether excluded volume interactions are included or no interactions are considered [34].

3.2. Drug release from slabs with rough surfaces

In a real situation the surfaces of a slab or a membrane are not perfectly flat, but they exhibit some degree of roughness. For example in the Fig. S2 of Supplementary information an optical profilometer image of a drug-loaded thin polymeric membrane is shown [35,36]. Of course the degree of roughness varies from case to case. In this section we numerically investigate the influence of surface roughness on the release profiles by considering irregular surfaces and examining different amplitudes w of surface fluctuations.

To mimic an experimental situation like that shown in Fig. S2 of Supplementary information, we have constructed rough surfaces using the procedure described in Subsection 2.2. Indicative examples of irregular surfaces obtained in this way are shown in Fig. 4. At the *left* (*right*) of this figure a three-dimensional plot (a two-dimensional contour plot) of the lower (upper) rough surface is displayed for a lattice with $N_x \times N_y$ equal to 20×20 (80×80), $n_s = 5$, average thickness $L = 60$ ($L = 100$) and amplitude of surface fluctuations $w = 8$.

Slabs with such irregular surfaces present a non-uniform thickness, with an average value L. The variation of the thickness ΔL is given through the amplitude w of surface fluctuations. For upper and lower non-planar surfaces with positions fluctuating in the interval $L \pm w$ and $0 \pm w$, respectively, the slab thickness varies in the range $L \pm \Delta L$, where $\Delta L = 2w$. For the surfaces considered in our simulations, the resulted slabs exhibit a thickness distribution resembling a Gaussian. These are demonstrated in Fig. 5: the

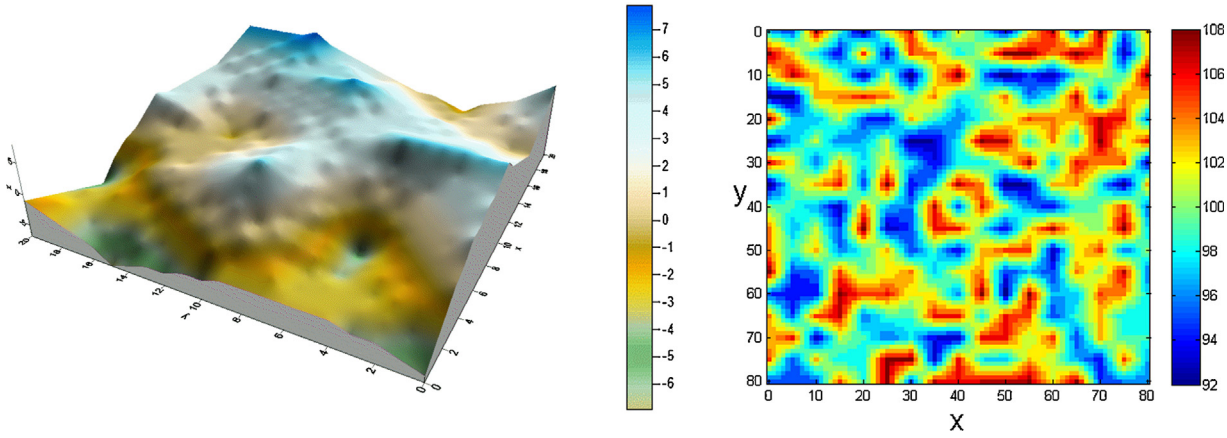

Fig. 4. Examples of numerically constructed rough surfaces. *Left*: Three-dimensional view of the lower surface of a lattice with $N_x \times N_y = 20 \times 20$, $n_s = 5$, average thickness $L = 60$, and amplitude of surface fluctuations $w = 8$. *Right*: Contour plot of the upper surface of a lattice with $N_x \times N_y = 80 \times 80$, $n_s = 5$, average thickness $L = 100$, and amplitude of surface fluctuations $w = 8$. The color bars at the right of each plot display the z coordinates of the lower and upper surface, respectively.

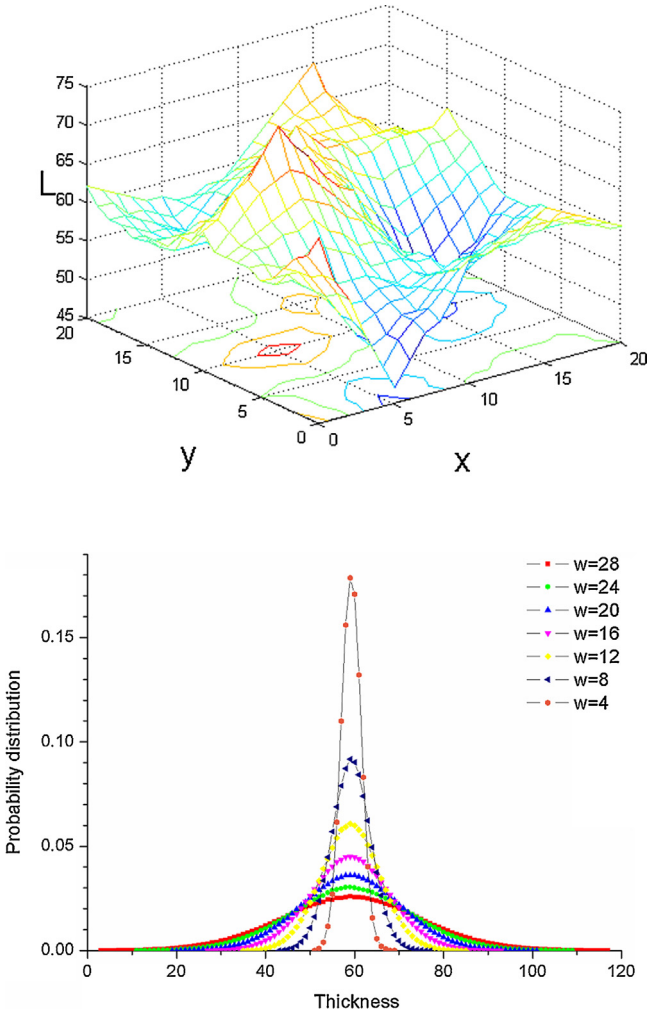

Fig. 5. Thickness variability of the slabs considered in our simulations. Top: Thickness variation of an indicative example of a slab with $N_x \times N_y = 20 \times 20$, $n_s = 5$, average thickness $L = 60$, and amplitude of surface fluctuations $w = 8$ (degree of thickness variability $\Delta L = 16$). Bottom: Thickness distributions for various values of w in

variation of the thickness in a particular simulation of one example of a slab with average thickness $L = 60$ and $w = 8$ ($\Delta L = 16$) is shown at the top, while the thickness distributions for different values of w at a fixed $L = 60$ is presented at the bottom. In the latter case, the distribution corresponding at each w is obtained over a few thousands of simulations at the particular values of w and L.

3.2.1. Release profiles obtained by Monte Carlo simulations

Numerical results of the release profiles, obtained through Monte Carlo simulations, for slabs with an average thickness $L = 60$ and different amplitudes w of surface roughness are presented in Fig. 6. Releases curves have been statistically averaged over a few thousands realizations. Standard deviations are not shown for clarity, but indicative errors can be seen in Fig. 7 below. For comparison we have also included in Fig. 6 the data for a slab with flat surfaces and a uniform thickness $L = 60$ (corresponding to the case $w = 0$). It can be seen that by increasing w, i.e., increasing the surface roughness, the drug release is substantially accelerated. Note that the more rough is the surface, the larger the area of the surface from where the drug is released.

Analogous results to those shown in Fig. 6 for $L = 60$ are also obtained for slabs with other average thicknesses, $L = 20$, 80, and 100. In each case w was varied from zero up to values just below $L/2$ (since $\Delta L = 2w$ should be less than L, otherwise holes would be created in the slab). It has been also checked that larger values of $N_x \times N_y$ give similar results.

The choice of the sub-grid spacing n_s, used in our method for constructing rough surfaces in the simulations (see Subsection 2.2 and the related Fig. S1 in the Supplementary information), affects the release kinetics. In particular, for a fixed value of w, by increasing n_s the release is delayed. This seems reasonable because the surfaces become smoother in this way; as the number of the sub-grid sites (i.e., the sites i,j of the $N_x \times N_y$ grid where the positions of the surfaces randomly fluctuate) is decreasing, while the intermediate grid sites between those ones correspond to smooth variations of surfaces' positions due to the bilinear interpolation. Therefore the degree of surface roughness is provided through a combination of the parameters w and n_s as follows: the larger the value of the amplitude of fluctuations w, or the smaller the sub-grid spacing n_s, the higher the surface roughness. Our numerical simulations indicate that a higher surface roughness gives faster release rates, while smoother surfaces delay the release. This property may be used for controlled release, especially in cases that smart systems inducing roughness would be devised.

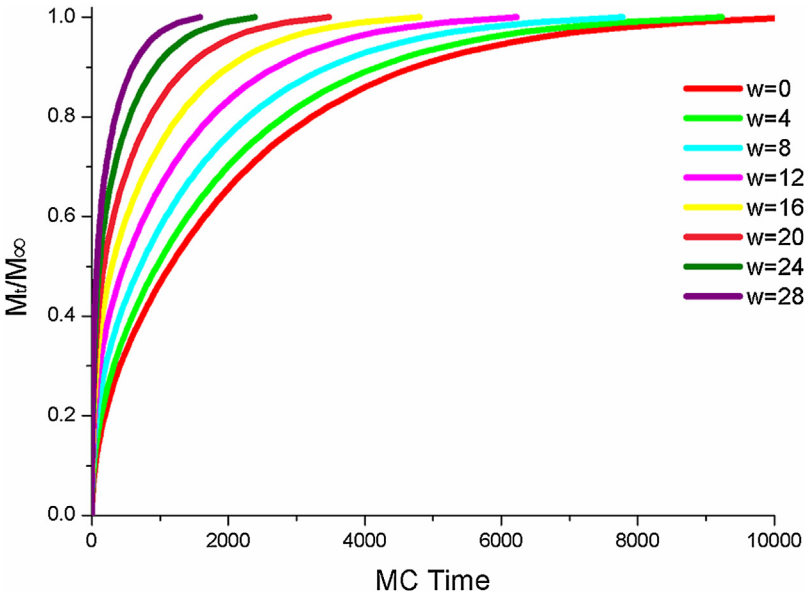

Fig. 6. Fractional drug release, M_t/M_∞, from slabs with rough surfaces, as a function of Monte Carlo time, for various amplitudes w of surface fluctuations. The case $w = 0$ corresponds to planar surfaces (slab of uniform thickness). In all cases slabs of $N_x \times N_y = 20 \times 20$, $n_s = 5$, and average thickness $L = 60$ are used.

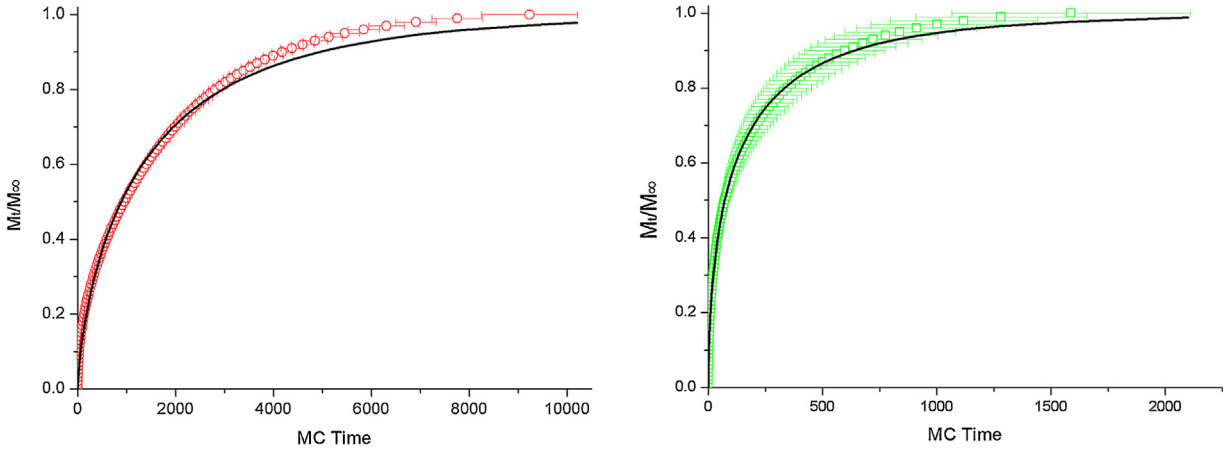

Fig. 7. Release profiles, M_t/M_∞, as a function of Monte Carlo time for the cases with $w = 4$ (circles, *left*) and $w = 28$ (squares, *right*) of Fig. 6. Error bars correspond to standard deviations from the different realizations. Continuous lines represent fits of the numerical results with the stretched exponential function, Eq. (1).

3.2.2. Dependence of stretched exponential parameters on the degree of thickness variability

In order to quantitatively describe the dependence of release kinetics on the degree of thickness variation, we have fitted the numerically obtained results with the stretched exponential function, Eq. (1). As in other cases, this simple analytical formula provides a good overall description of the fractional release. This can be seen from Fig. 7, where the fitting of the release profiles of Fig. 6 corresponding to $w = 4$ (red circles in Fig. 7) and $w = 28$ (green squares in Fig. 7) is shown by solid lines. Concerning the data from the numerical simulations in this figure, note that the relative errors are significantly larger as w increases, due to the increased irregularity of the surfaces.

Through fittings like those shown in Fig. 7, the values of the stretched exponential parameters b and τ are obtained for each case examined. The dependence of these parameters on the degree of thickness variability $\Delta L = 2w$ is presented in Fig. 8, for two different average slab thicknesses, $L = 60$ (circles) and $L = 100$ (triangles). The data at $\Delta L = 0$ correspond to $w = 0$, i.e., to slabs with a uniform thickness $L = 60$ or $L = 100$, respectively (see the values of τ and b shown in Fig. 3).

We see that the time parameter τ decreases with ΔL (Fig. 8, *left*), showing this behavior up to the maximum allowed value of thickness variability ($\Delta L < L$). On the contrary, the stretched exponential exponent b displays a non-monotonous dependence (Fig. 8, *right*), presenting a minimum at a value of ΔL around $(2/3)L$.

4. Conclusions

We have examined drug release from slabs/thin films of either flat, or rough, surfaces and discussed the influence of surface roughness on release kinetics. Monte Carlo simulations are used for the numerical calculation of diffusion-controlled release profiles. Analytical results are considered in the case of slabs with uniform thickness. Fractional release has been quantified through the stretched exponential function and the dependence of the two

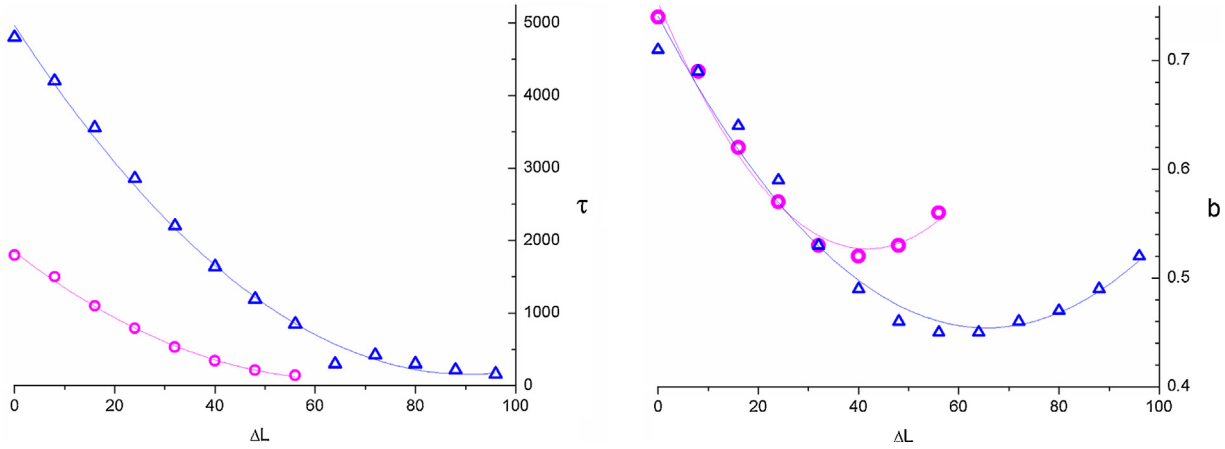

Fig. 8. Dependence of the stretched exponential parameters on the degree of thickness variability ΔL. *Left*: Time parameter τ as a function of ΔL. *Right*: Exponent b as a function of ΔL. Triangles correspond to slabs with average thickness $L = 100$, and circles to $L = 60$. In all cases $N_x \times N_y = 20 \times 20$ and $n_s = 5$. Solid lines show fits with polynomials of second degree.

parameters of this function on the relevant characteristics of the system.

In the case of slabs with planar surfaces, the predictions from the analytical solution of diffusion equation are first discussed, regarding the dependence of the stretched exponential time parameter τ and the exponent b on the thickness of the device and the diffusion coefficient. Then these predictions have been confirmed by the numerical results obtained through Monte Carlo simulations. Both approaches show the same dependencies, with only small differences on the values of the numerical constants.

Slabs with rough surfaces, exhibiting non-uniform thickness, have been investigated through numerical simulations. For this purpose a method for constructing irregular surfaces was developed. Films of different average thickness and for various degrees of surface roughness have been examined. We found that the higher the roughness, the faster the release, while the release rate is slowing down for smoother slab surfaces. The dependence of the stretched exponential parameters on the degree of thickness variability ΔL is presented. While the time parameter τ decreases monotonously with ΔL, the exponent b shows a richer behavior presenting a minimum.

Acknowledgements

We thank Dr N. Bouropoulos and I. Kontopoulou for providing the experimental Fig. S2 shown in the Supplementary information. This work has been partially supported by the Thales project MACOMSYS, co-financed by the European Union (ESF) and the Greek Ministry of Education (through the EΣΠΑ program), and by European Union's Seventh Framework Programme (FP7-REGPOT-2012-2013-1) under grant agreement no. 316165.

Appendix A. Supplementary data

Supplementary data associated with this article can be found, in the online version, at http://dx.doi.org/10.1016/j.ijpharm.2015.10.018.

References

Picheth, G.F., Sierakowski, M.R., Woehl, M.A., Ono, L., Cofre, A.R., Vanin, L.P., Pontarolo, R., De Freitas, R.A., [1]. Lysozyme-triggered epidermal growth factor release from bacterial cellulose membranes controlled by smart nanostructured films. J. Pharm. Sci. 103, 3958–3965.
Bhattacharyya, S., Agrawal, A., Knabe, C., Ducheyne, P., [2]. Sol–gel silica controlled release thin films for the inhibition of methicillin-resistant *Staphylococcus aureus*. Biomaterials 35, 509–517.
Sundararaj, S.C., Thomas, M.V., Peyyala, R., Dziubla, T.D., Puleo, D.A., [3]. Design of a multiple drug delivery system directed at periodontitis. Biomaterials 34, 8835–8842.
Soulas, D.N., Sanopoulou, M., Papadokostaki, K.G., [4]. Proxyphylline release kinetics from symmetrical three-layer silicone rubber matrices: effect of different excipients in the outer rate-controlling layers. Int. J. Pharm. 427, 192–200.
Higuchi, T., [5]. Rate of release of medicaments from ointment bases containing drugs in suspensions. J. Pharm. Sci. 50, 874–875.
Siepmann, J., Peppas, N.A., [6]. Higuchi equation: derivation, applications, use and misuse. Int. J. Pharm. 418, 6–12.
Lin, C.-C., Metters, A.T., [7]. Hydrogels in controlled release formulations: network design and mathematical modeling. Adv. Drug Deliv. Rev. 58, 1379–1408.
Siepmann, J., Siepmann, F., [8]. Mathematical modeling of drug delivery. Int. J. Pharm. 364, 328–343.
Lao, L.L., Peppas, N.A., Boey, F.Y.C., Venkatraman, S.S., [9]. Modeling of drug release from bulk-degrading polymers. Int. J. Pharm. 418, 28–41.
Siepmann, J., Siepmann, F., [10]. Modeling of diffusion controlled drug delivery. J. Control. Release 161, 351–362.
Peppas, N.A., Narasimhan, B., [11]. Mathematical models in drug delivery: how modeling has shaped the way we design new drug delivery systems. J. Control. Release 190, 75–81.
Ritger, P.L., Peppas, N.A., [12]. A simple equation for description of solute release I. Fickian and non-Fickian release from non-swellable devices in the form of slabs, spheres, cylinders or discs. J. Control. Release 5, 23–36.
Ritger, P.L., Peppas, N.A., [13]. A simple equation for description of solute release II. Fickian and anomalous release from swellable devices. J. Control. Release 5, 37–42.
Muschert, S., Siepmann, F., Leclercq, B., Carlin, B., Siepmann, J., [14]. Prediction of drug release from ethylcellulose coated pellets. J. Control. Release 135, 71–79.
Peppas, N.A., Gurny, R., Doelker, E., Buri, P., [15]. Modelling of drug diffusion through swellable polymeric systems. J. Membr. Sci. 7, 241–253.
Korsmeyer, R.W., Lustig, S.R., Peppas, N.A., [16]. Solute and penetrant diffusion in swellable polymers I. Mathematical modeling. J. Polym. Sci. B Polym. Phys. 24, 395–408.
Brazel, C.S., Peppas, N.A., [17]. Modeling of drug release from swellable polymers. Eur. J. Pharm. Biopharm. 49, 47–58.
Thombre, A.G., Himmelstein, K.J., [18]. Modelling of drug release kinetics from a laminated device having an erodible drug reservoir. Biomaterials 5, 250–254.
Joshi, A., Himmelstein, K.J., [19]. Dynamics of controlled release from bioerodible matrices. J. Control. Release 15, 95–104.
Prabhu, S., Hossainy, S., [20]. Modeling of degradation and drug release from a biodegradable stent coating. J. Biomed. Mater. Res. A 80, 732–741.
Casault, S., Slater, G.W., [21]. Comments concerning: Monte Carlo simulations for the study of drug release from matrices with high and low diffusivity areas. Int. J. Pharm. 365, 214–215.
Papadopoulou, V., Kosmidis, K., Vlachou, M., Macheras, P., [22]. On the use of the Weibull function for the discernment of drug release mechanisms. Int. J. Pharm. 309, 44–50.
Spanakis, M., Bouropoulos, N., Theodoropoulos, D., et al., [23]. Controlled release of 5-fluorouracil from microporous zeolites. Nanomed. NBM 10, 197–205.
Kosmidis, K., Argyrakis, P., Macheras, P., [24]. A reappraisal of drug release laws using Monte Carlo simulations: the prevalence of the Weibull function. Pharm. Res. 20, 988–995.
Kosmidis, K., Argyrakis, P., Macheras, P., [25]. Fractal kinetics in drug release from finite fractal matrices. J. Chem. Phys. 119, 6373–6377.
Macheras, P., Iliadis, A., [26]. Modeling in Biopharmaceutics, Pharmacokinetics, and Pharmacodynamics: Homogeneous and Heterogeneous Approaches. Springer, New York.

Villalobos, R., Vidales, A.M., Cordero, S., Quintanar, D., Domnguez, A., [27]. Monte Carlo simulation of diffusion-limited drug release from finite fractal matrices. J. Sol–Gel Sci. Technol. 37, 195–199.
Villalobos, R., Cordero, S., Vidales, A.M., Domínguez, A., [28]. In silico study on the effects of matrix structure in controlled drug release. Phys. A 367, 305–318.
Kosmidis, K., Macheras, P., [29]. Monte Carlo simulations for the study of drug release from matrices with high and low diffusivity areas. Int. J. Pharm. 343, 166–172.
Kosmidis, K., Macheras, P., [30]. Monte Carlo simulations of drug release from matrices with periodic layers of high and low diffusivity. Int. J. Pharm. 354, 111–116.
Martínez, L., Villalobos, R., Sánchez, M., Cruz, J., Ganem, A., Melgoza, L.M., [31]. Monte Carlo simulations for the study of drug release from cylindrical matrix systems with an inert nucleus. Int. J. Pharm. 369, 38–46.
Hadjitheodorou, A., Kalosakas, G., [32]. Quantifying diffusion-controlled drug release from spherical devices using Monte Carlo simulations. Mater. Sci. Eng. C 33, 763–768.
Hadjitheodorou, A., Kalosakas, G., [33]. Analytical and numerical study of diffusion-controlled drug release from composite spherical matrices. Mater. Sci. Eng. C 42, 681–690.
Bunde, A., Havlin, S., Nossal, R., Stanley, H.E., Weiss, G.H., [34]. On controlled diffusion-limited drug release from a leaky matrix. J. Chem. Phys. 83, 5909–5913.
I. Kontopoulou, N. Bouropoulos, unpublished.
Kontopoulou, I., [36]. Physicochemical characterization and study of bioactive compound release from biocompatible polymeric matrices. Diploma Thesis (in Greek) .

Supplementary information

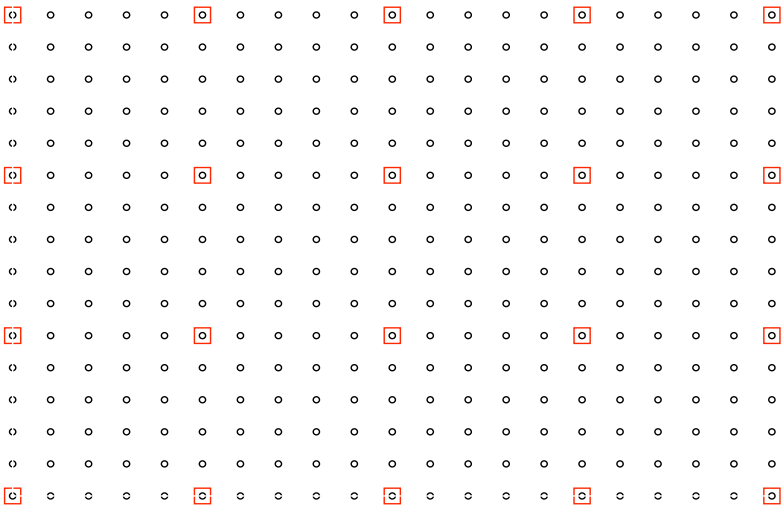

Figure S1. Schematic representation of the procedure used for the construction of rough surfaces in the numerical simulations. The sub-grid shown by red squares corresponds to the positions of the xy-plane where randomly selected integer numbers (in the range $0 \pm w$ for the lower surface and $L \pm w$ for the upper surface) provide the z coordinates of slab's main surfaces. The integer z coordinates of the lower and upper surfaces at the other points of the grid (shown by black circles) have been calculated using bilinear interpolation between the random values of the sub-grid.

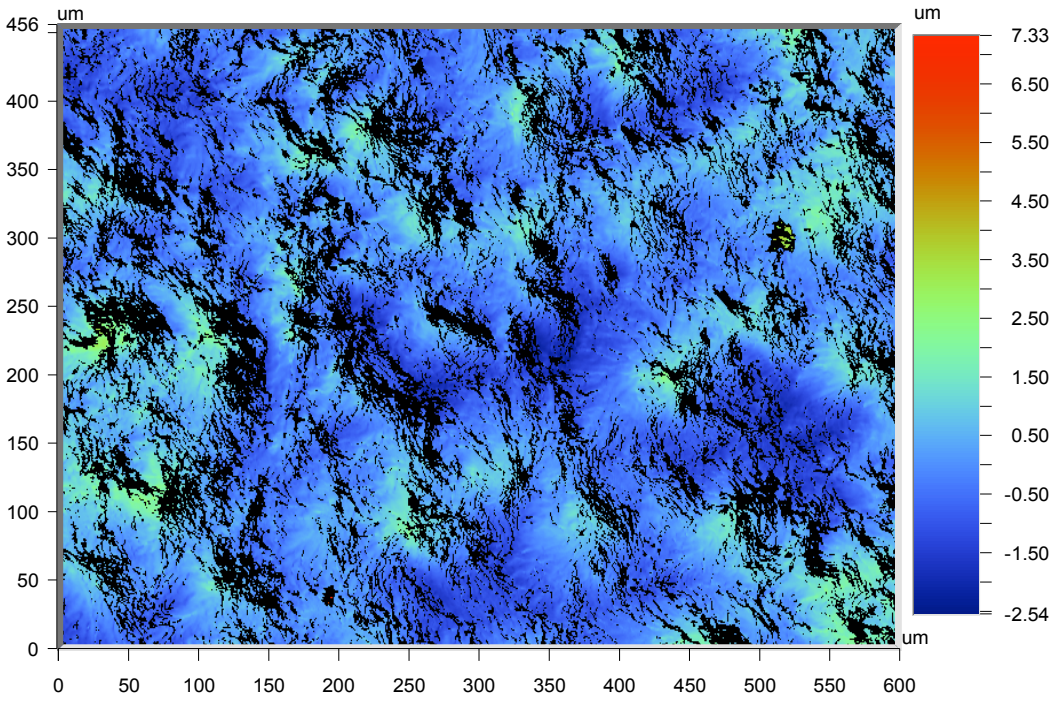

Figure S2. Optical profilometer image of a thin poly(ε-caprolactone) membrane loaded with 0.2% Verapamil Hydrochloride. A surface region with dimensions around 600x450 μm is shown. The colorbar at the right displays the fluctuations of the surface roughness. The average thickness is around 2.7 mm in this case. (*Courtesy of I. Kontopoulou and N. Bouropoulos*).